

# **U**nsolved **P**roblems of **M**agnetospheric **P**hysics

WORKSHOP • SCARBOROUGH, UK • SEPTEMBER 2015

## Unsolved Problems In Ionospheric Conductivity

Daniel Weimer  
Virginia Tech

While the basic physics of ionospheric conductivity are known, the formulas are often written in different ways:

M. (Fred) H. Rees [1989]

complete conductivity coefficient for the Birkeland current parallel to the magnetic field is

$$\sigma_0 = \frac{e^2 n_e}{m_e (v_{en} + v_{ei})} + \sum_i \frac{e^2 n_i}{m_i v_{in}} \quad (8.3.18)$$

which includes the electron–ion collision frequency,  $v_{ei}$ . Electron–ion collisions become important at high ionospheric levels where the degree of ionization is large.

$$\sigma_{\perp} = \sum_i \frac{en_i}{B} \left( \frac{v_{en} \omega_{ce}}{\omega_{ce}^2 + v_{en}^2} + \frac{v_{in} \omega_{ci}}{\omega_{ci}^2 + v_{in}^2} \right) \quad (8.3.20)$$

$$\sigma_H = \sum_i \frac{en_i}{B} \left( \frac{\omega_{ce}^2}{\omega_{ce}^2 + v_{en}^2} - \frac{\omega_{ci}^2}{\omega_{ci}^2 + v_{in}^2} \right) \quad (8.3.21)$$

$k_i = \Omega_i/v_{in}$  is the ion mobility coefficient when  $\Omega_i = eB/m_i$

$$\sigma_P = \frac{n_e \cdot e}{B} \left( \frac{k_e}{1 + k_e^2} + \frac{k_i}{1 + k_i^2} \right)$$

$$\sigma_H = \frac{n_e \cdot e}{B} \left( \frac{k_e^2}{1 + k_e^2} - \frac{k_i^2}{1 + k_i^2} \right)$$

$$\sigma_{\parallel} = \frac{ne \cdot e}{B} (k_e + k_i)$$

(above) [A. Brekke \[2013\]](#)

(below) [Gurnett and Bhattacharjee \[2005\]](#)

$$\sigma_s = \frac{n_s e_s^2}{m_s \nu_s} \quad (5.6.8)$$

$$\vec{\sigma} = \begin{bmatrix} \sigma_{\perp} & \sigma_H & 0 \\ -\sigma_H & \sigma_{\perp} & 0 \\ 0 & 0 & \sigma_{\parallel} \end{bmatrix}, \quad (5.6.12)$$

where

$$\sigma_{\perp} = \sum_s \frac{\sigma_s}{(1 + \omega_{cs}^2/\nu_s^2)}, \quad \sigma_H = \sum_s \frac{\sigma_s (\omega_{cs}/\nu_s)}{(1 + \omega_{cs}^2/\nu_s^2)} \quad (5.6.13)$$

and  $\sigma_{\parallel} = \sum_s \sigma_s$ .

$$\nu_{ei} = [34 + 4.18 \ln(T_e^3/n_e)] n_e T_e^{-3/2} \text{ s}^{-1}$$

$$\sigma_0 = ne^2 (1/m\nu_e + 1/M\nu_i)$$

$$\sigma_p = ne^2 \left( \frac{\nu_e}{m(\nu_e^2 + \Omega_e^2)} + \frac{\nu_i}{M(\nu_i^2 + \Omega_i^2)} \right)$$

$$\sigma_H = ne^2 \left( \frac{\Omega_i}{M(\nu_i^2 + \Omega_i^2)} - \frac{\Omega_e}{m(\nu_e^2 + \Omega_e^2)} \right)$$

(above) [M.C. Kelley \[1989\]](#),  
is the same form as by  
[Su. Basu \[1985\]](#)

(in *Air Force Handbook of Geophysics  
and the Space Environment*)

Other variations of these  
equations have been seen.

## To calculate the ionospheric conductivities you need to know:

- magnetic field strength
- neutral composition
- temperature
- ion/electron densities

And to get these, you also need to know:

- sunlight ionization rates and equilibrium densities
- ion production rates from precipitating particles
- recombination rates
- plasma drift from day to nightside (cannot do in 1D)

# M.C. Kelley [1989]

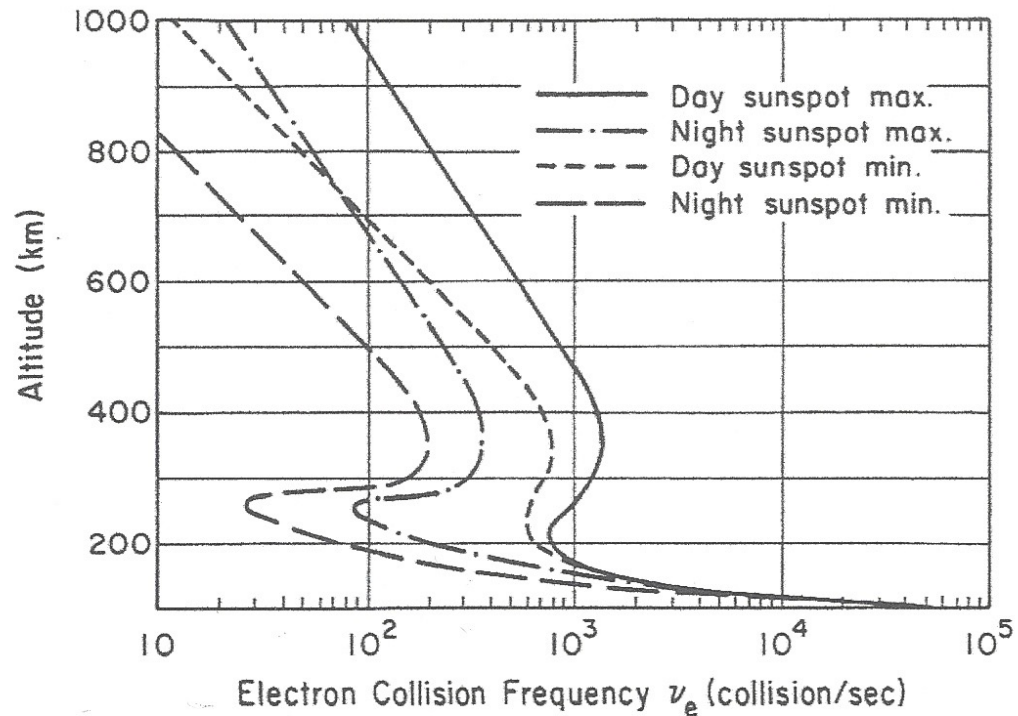


Fig. B.3. Electron collision frequency versus altitude. [From Johnson (1961).]

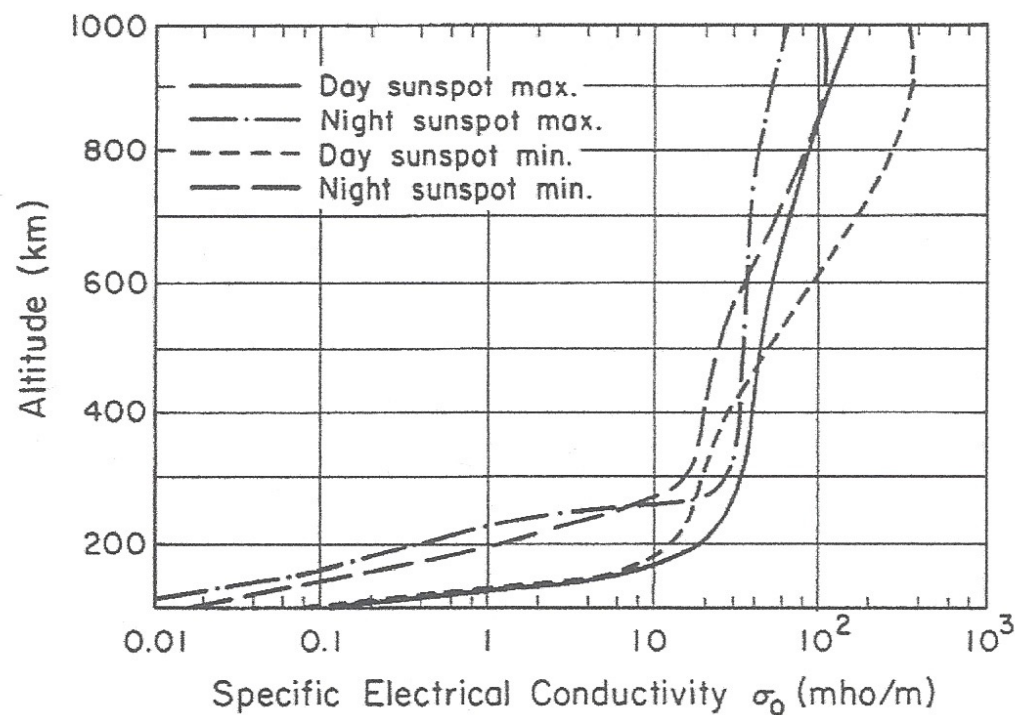


Fig. B.4. Parallel electrical conductivity  $\sigma_0$  (zero-field conductivity) versus altitude. [From Johnson (1961).]

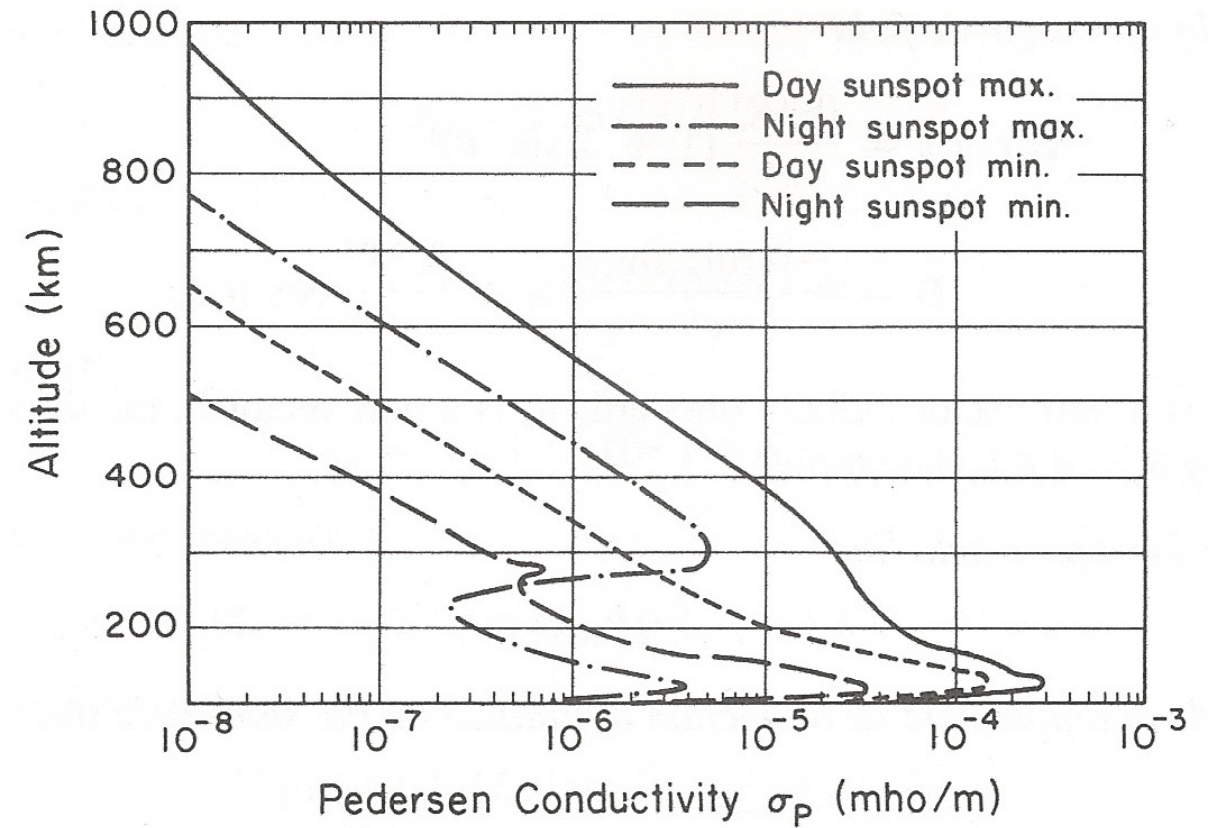


Fig. B.5. Pedersen conductivity versus altitude. [From Johnson (1961).]

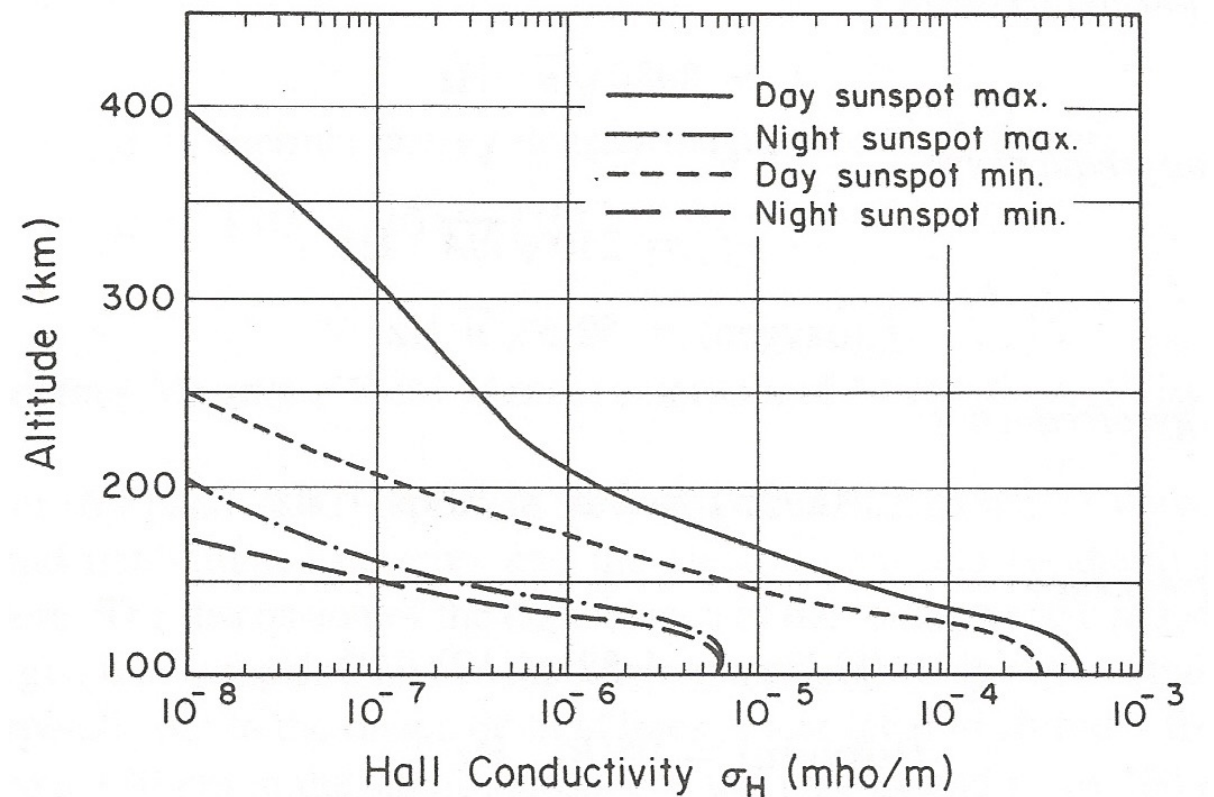


Fig. B.6. Hall conductivity versus altitude. [From Johnson (1961).]

# The Solar Contribution

Richmond [1995]

$$\Sigma_P^{EUV} = 11 \left( \frac{F_{10.7}}{100} \right)^{1.1} \left( \frac{B}{50 \mu T} \right)^{-1.6} (\cos \chi)^{0.5}$$

$$\Sigma_H^{EUV} = 14 \left( \frac{F_{10.7}}{100} \right)^{0.5} \left( \frac{B}{50 \mu T} \right)^{-1.3} (\cos \chi)^{0.8}$$

Wiltberger et al. [2004], said to be used in AMIE, Richmond and Kamide [1998]

$$\Sigma_P = 0.5 F_{10.7}^{2/3} \cos(\chi)^{2/3} \quad \chi \leq 65^\circ,$$

$$\Sigma_P = \Sigma_P^{65^\circ} - 0.12 F_{10.7}^{2/3} (\chi - 65^\circ) \quad 65^\circ < \chi \leq 100^\circ,$$

$$\Sigma_P = \Sigma_P^{100^\circ} - 0.065 F_{10.7}^{2/3} (\chi - 100^\circ) \quad \chi > 100^\circ$$

and Hall

$$\Sigma_H = 1.8 F_{10.7}^{1/2} \cos(\chi) \quad \chi \leq 65^\circ,$$

$$\Sigma_H = \Sigma_H^{65^\circ} - 0.49 F_{10.7}^{1/2} (\chi - 65^\circ) \quad \chi > 65^\circ,$$

Moen and Brekke [1992]

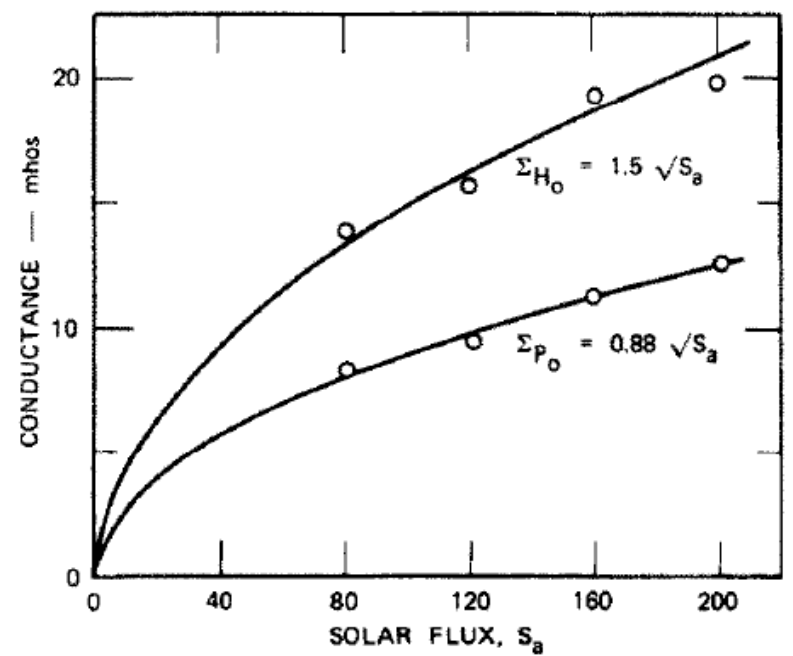
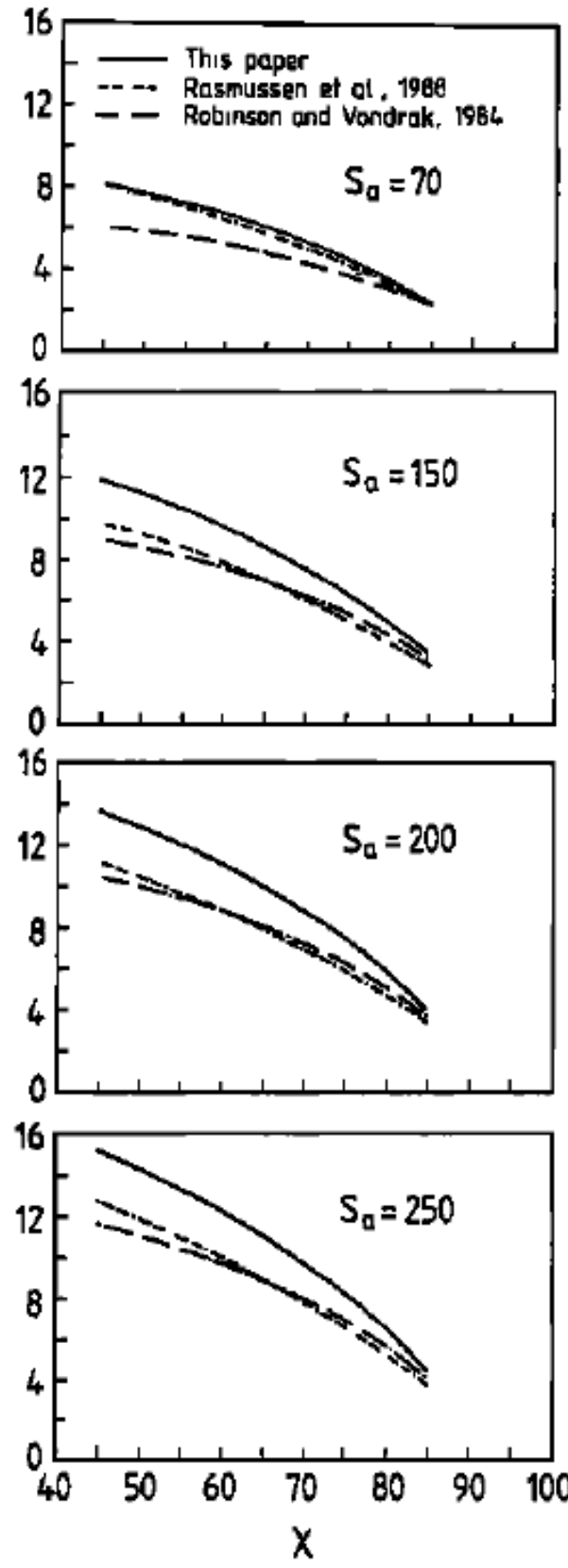


Fig. 9. Height integrated Hall and Pedersen conductances as function of the solar flux ( $S_a$ ) given in units of  $10^{-22} \text{ W m}^{-2} \text{ Hz}^{-1}$  as measured on 10.7 cm wavelength at Ottawa and adjusted to 1 A.U. (from ROBINSON and VONDRAK, 1984).

↕ Brekke and Moen [1993]

Author	Year	$\Sigma_P$	$\Sigma_H$
Schuster	1889, 1908		$a + b \cdot \cos \chi$
Appleton	1937		$\text{const.} \cdot (\cos \chi)^{3/2} (v \gg \omega)$
Metha	1978	$7.1 \cdot (\cos \chi)^{0.44}$	$13.7 (\cos \chi)^{0.45}$
Senior	1980	$9.6 \cdot \cos \chi + 1.6$	$15.8 \cdot \cos \chi + 2.3$
Vickrey et al.	1981	$5 \cdot (\cos \chi)^{1/2}$	$10 \cdot (\cos \chi)^{1/2}$
de la Beaujardière et al.	1982	$10 \cdot \cos \chi + 2$	$16 \cdot \cos \chi + 3$
Robinson and Vondrak*	1984	$0.88 \sqrt{S_a} (\cos \chi)^{1/2}$	$1.5 \sqrt{S_a} (\cos \chi)^{1/2}$
Rasmussen et al.†	1988	$(4.5/B)(1 - 0.85 \cdot v^2) \cdot (1 + 0.15u + 0.05u^2)$	$(5.6/B) \cdot (1 - 0.9v^2) \cdot (1 + 0.15u + 0.005u^2)$
Schlegel	1988	$6.4 \cdot (\cos(\chi - 12^\circ))^{0.54}$	
Brekke and Hall	1988	$3.05 \cos \chi + 4.06 (\cos \chi)^{1/2}$	$6.24 \cos \chi + 2.85 (\cos \chi)^{1/2}$
Senior	1991	$1.81 + 8.88 \cos \chi$	$21.58 - 0.21 \cdot \chi$
Moen and Brekke	1992	$S_a^{0.49} \cdot (0.34 \cos \chi + 0.93 \cdot (\cos \chi)^{1/2})$	$S_a^{0.53} (0.81 \cos \chi + 0.54 (\cos \chi)^{1/2})$

\*  $S_a$  being the daily 10.7 cm solar radio flux at Ottawa in units of  $10^{-22} \text{ W m}^{-2} \text{ Hz}^{-1}$  (adjusted to 1 A.U.).  
 †  $v$  is the normalized zenith angle,  $v = \chi/90^\circ$ ,  $u$  is the normalized solar flux,  $u = S_a/90$ .  $B$  is the magnetic field strength.

# The Solar Contribution (continued)

Ridley et al. [2004] add scattering to smooth conductance across the terminator

The solar component can be approximated as (Moen and Brekke, 1993):

$$\Sigma_H = F_{10.7}^{.53} (0.81 \cos(\zeta) + 0.54 \sqrt{\cos(\zeta)}) \quad (11)$$

$$\Sigma_P = F_{10.7}^{.49} (0.34 \cos(\zeta) + 0.93 \sqrt{\cos(\zeta)}), \quad (12)$$

where  $F_{10.7}$  is the solar flux intensity at 10.7 cm, and  $\zeta$  is the solar zenith angle.

Plate 4 shows simulation results in which there are only 3 sources of conductance: (1) solar EUV, (2) scattering of the sunlight across the terminator and (3) nightside “starlight” conductance. The nightside Pedersen conductance is estimated to be 0.25 mhos, which dominates on the nightside (neglecting the aurora, as is done here). The solar EUV strongly dominates on the dayside. All conductances within the code are summed together using a vector summation. For example, the total Hall conductance discussed below is:

$$\Sigma_H = \sqrt{\Sigma_{HEUV}^2 + \Sigma_{HScat}^2 + \Sigma_{HSL}^2}, \quad (13)$$

where  $\Sigma_{HEUV}$  is the solar EUV Hall conductance (i.e. Moen and Brekke, 1993),  $\Sigma_{HScat}$  is the scattered sunlight Hall conductance, and  $\Sigma_{HSL}$  is the starlight Hall conductance.

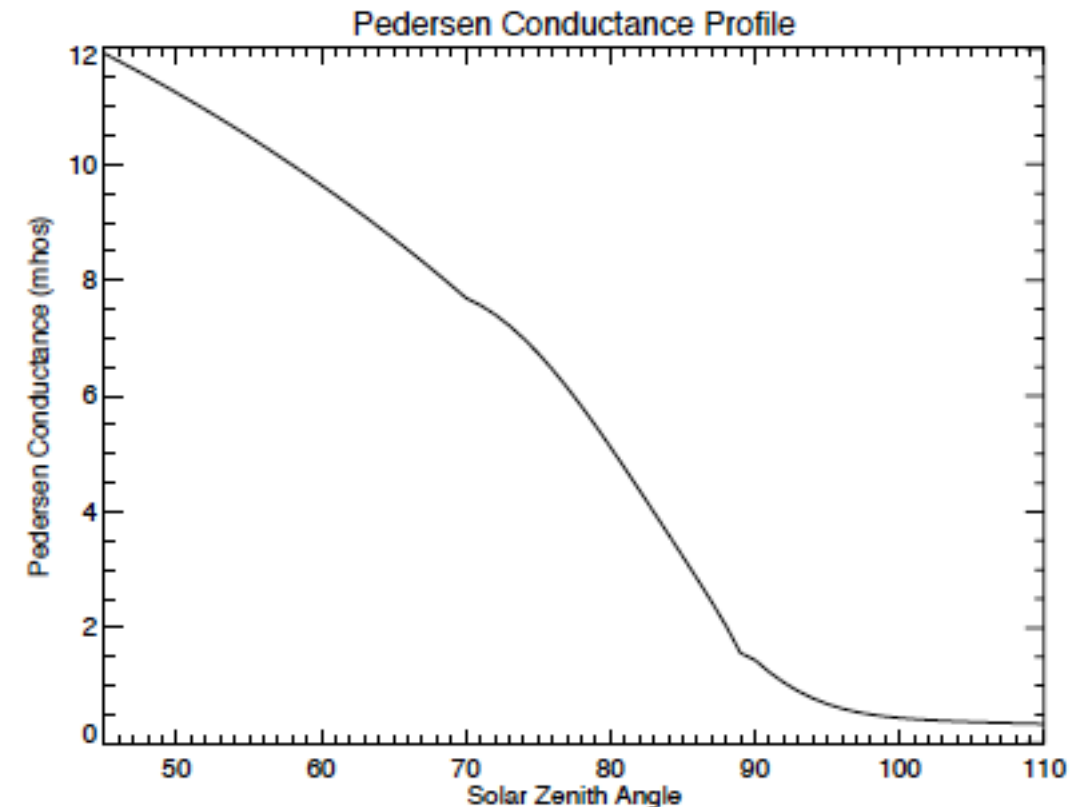
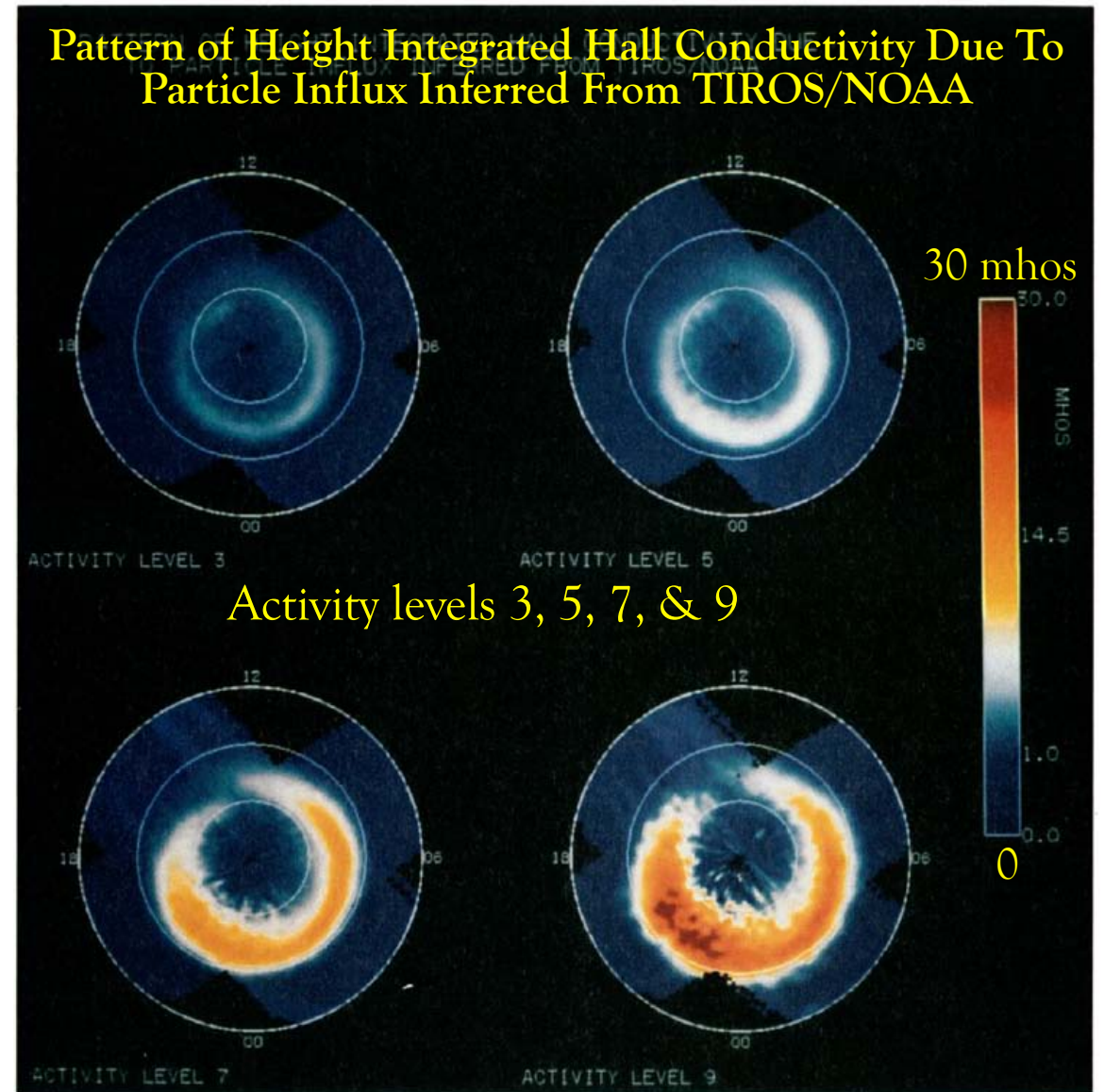
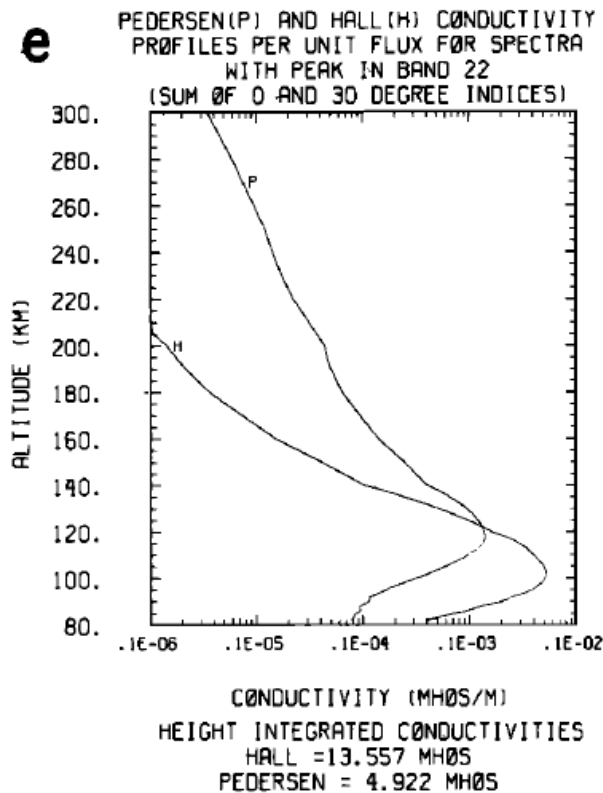
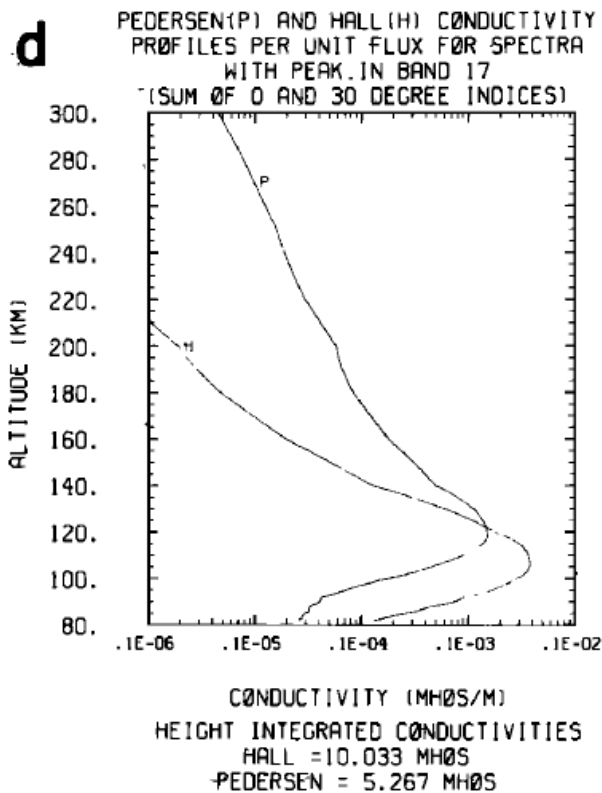
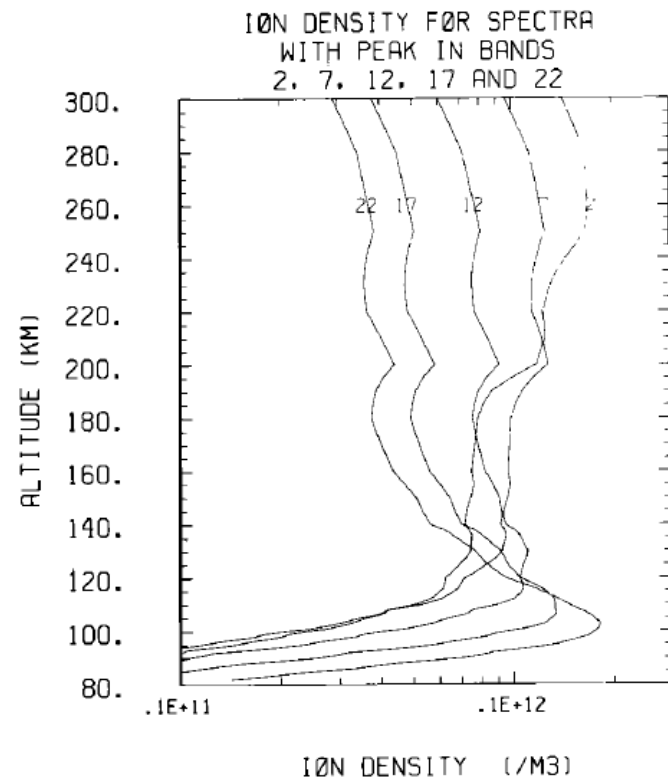
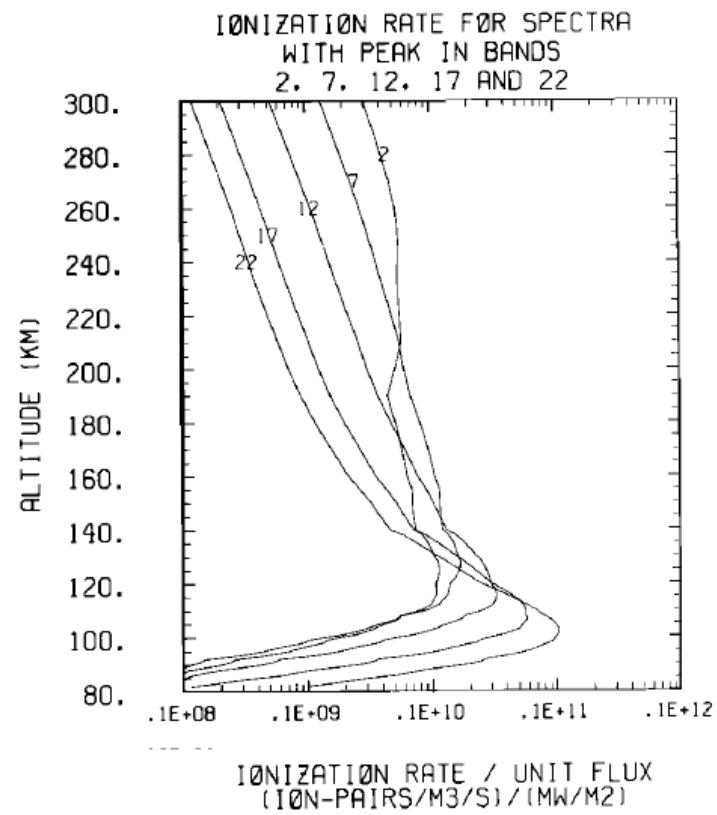


**Fig. 2.** A plot of the Pedersen conductance as a function of solar zenith angle. This shows the solar driven conductance, a scattering term which causes the conductance to be smoother across the terminator, and a nightside constant conductance. The squares of the conductances are added and the square root is taken to derive the total Pedersen conductance.

Fuller-Rowell and Evans [1987] used electron energy influx and energies from TIROS-NOAA satellites to build statistical patterns of these data and the derived Pedersen and Hall conductivities, ordered by an auroral activity index.



The Auroral Contribution

A similar to method was used by Hardy et al. [1987], using a statistical model of electron flux from DMSP measurements, sorted by the Kp index.

Hardy et al. used empirical formulas derived from numerical computations by Robinson et al. [1987],  relating the conductances to average energy and energy flux of the electrons:

$$\Sigma_P = \frac{40\bar{E}}{16 + \bar{E}^2} \Phi_E^{1/2}$$

$$\frac{\Sigma_H}{\Sigma_P} = 0.45(\bar{E})^{0.85}$$

average energy is in keV,  
and energy flux in  $\text{ergs}/\text{cm}^2 - \text{sec}$

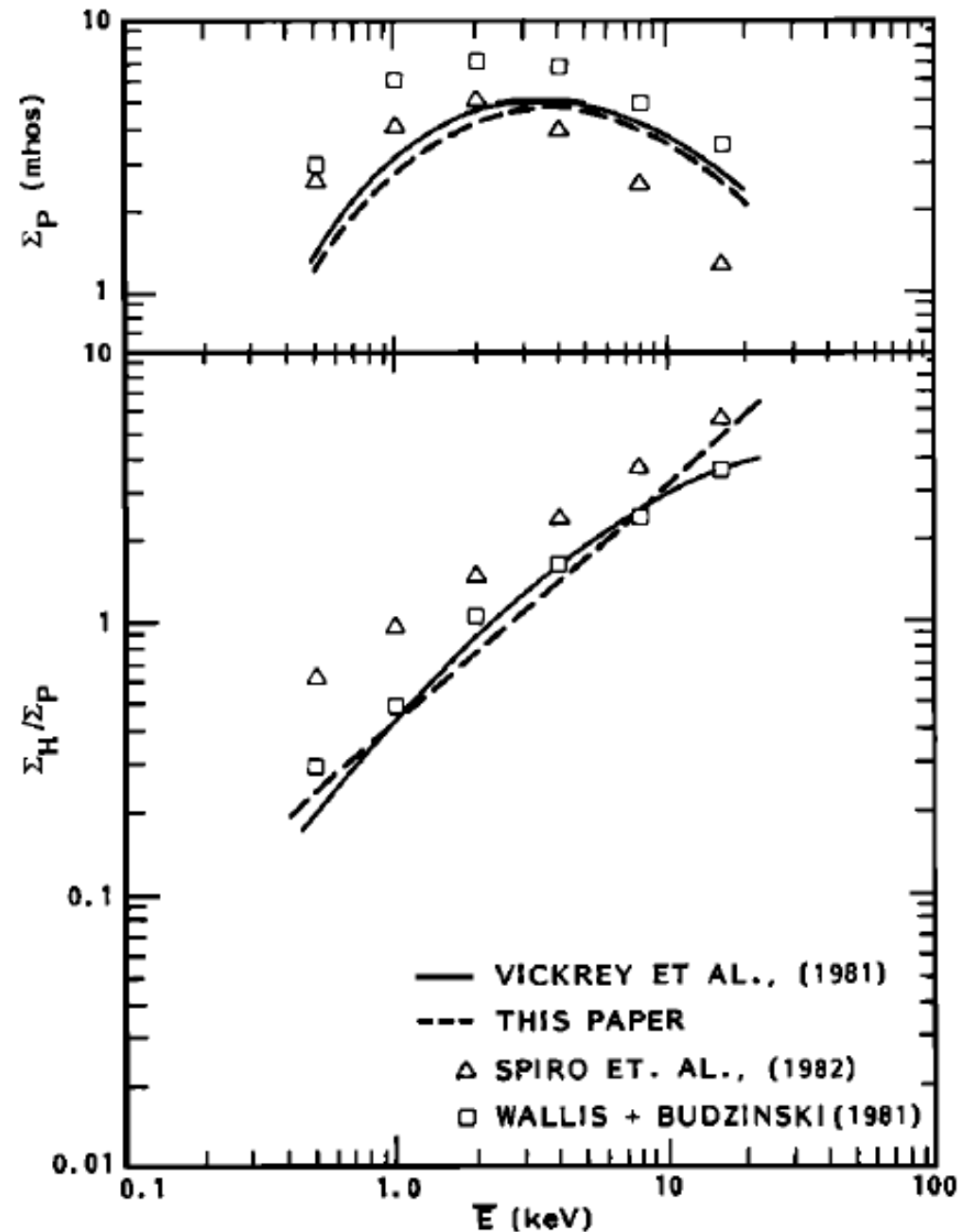
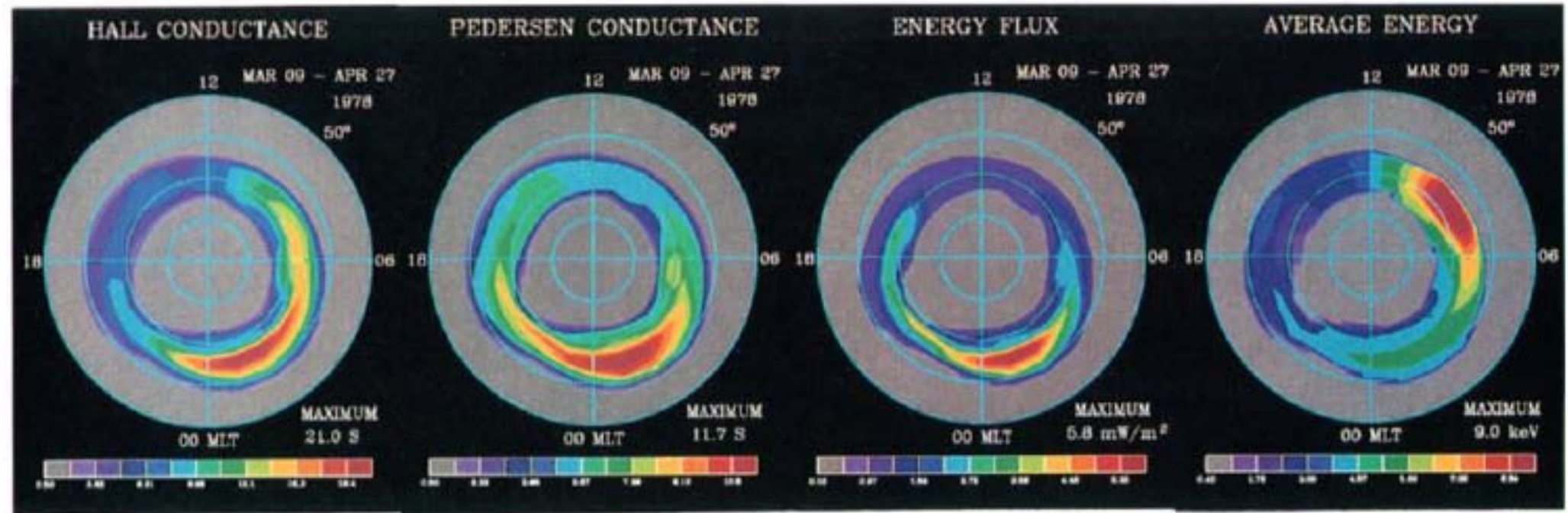


Fig. 1. Comparison of relations between conductances and the average energy of a Maxwellian distribution with an energy flux of  $1 \text{ ergs}/\text{cm}^2 \text{ s}$ . The results of Vickrey et al. [1981] represent those obtained using an energy deposition code. The results shown by dashed lines are those given by equations (3) and (4) of this paper.

Ahn et al. [1983, 1998] used radar measurements of conductivity and ground observations of magnetic perturbations to derive empirical relationships, then use delta-B to obtain global maps.

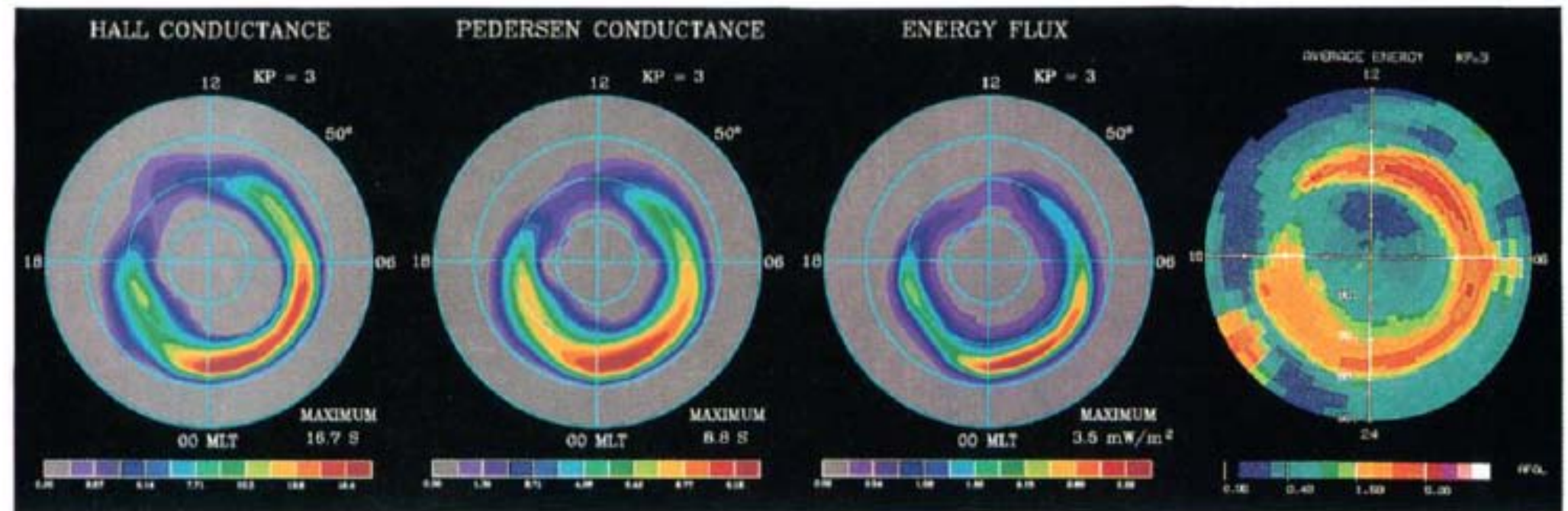


(a)

(c)

(e)

(g)



(b)

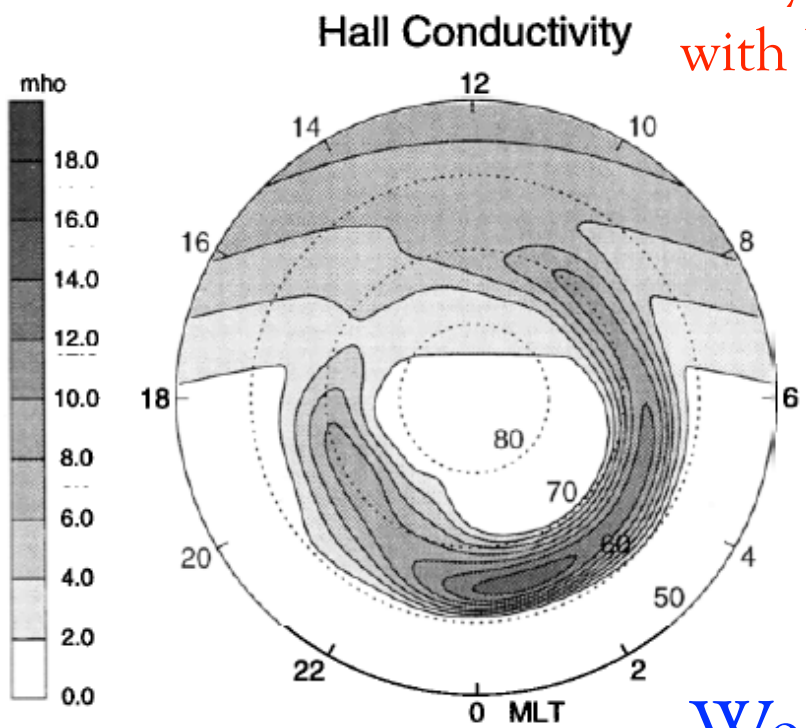
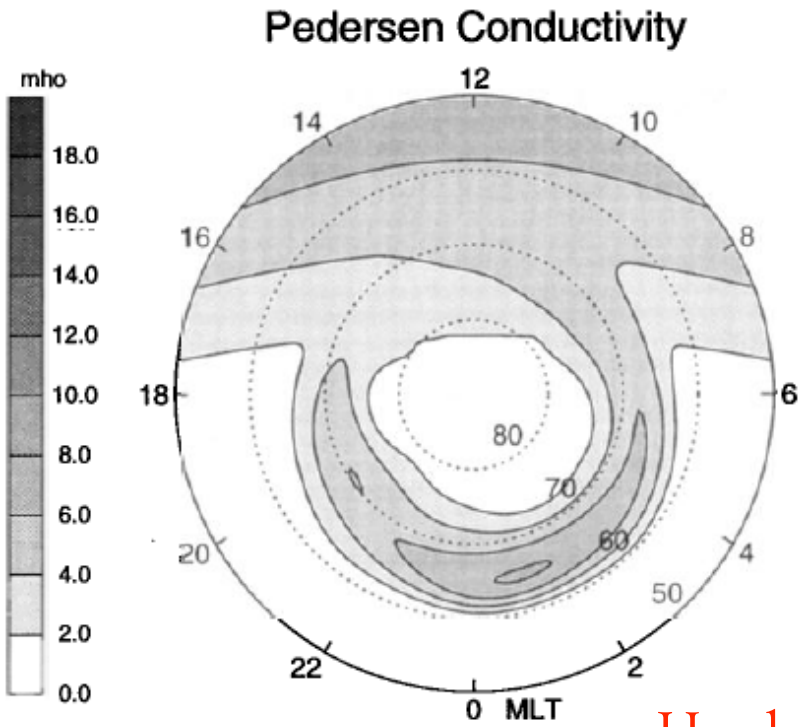
(d)

(f)

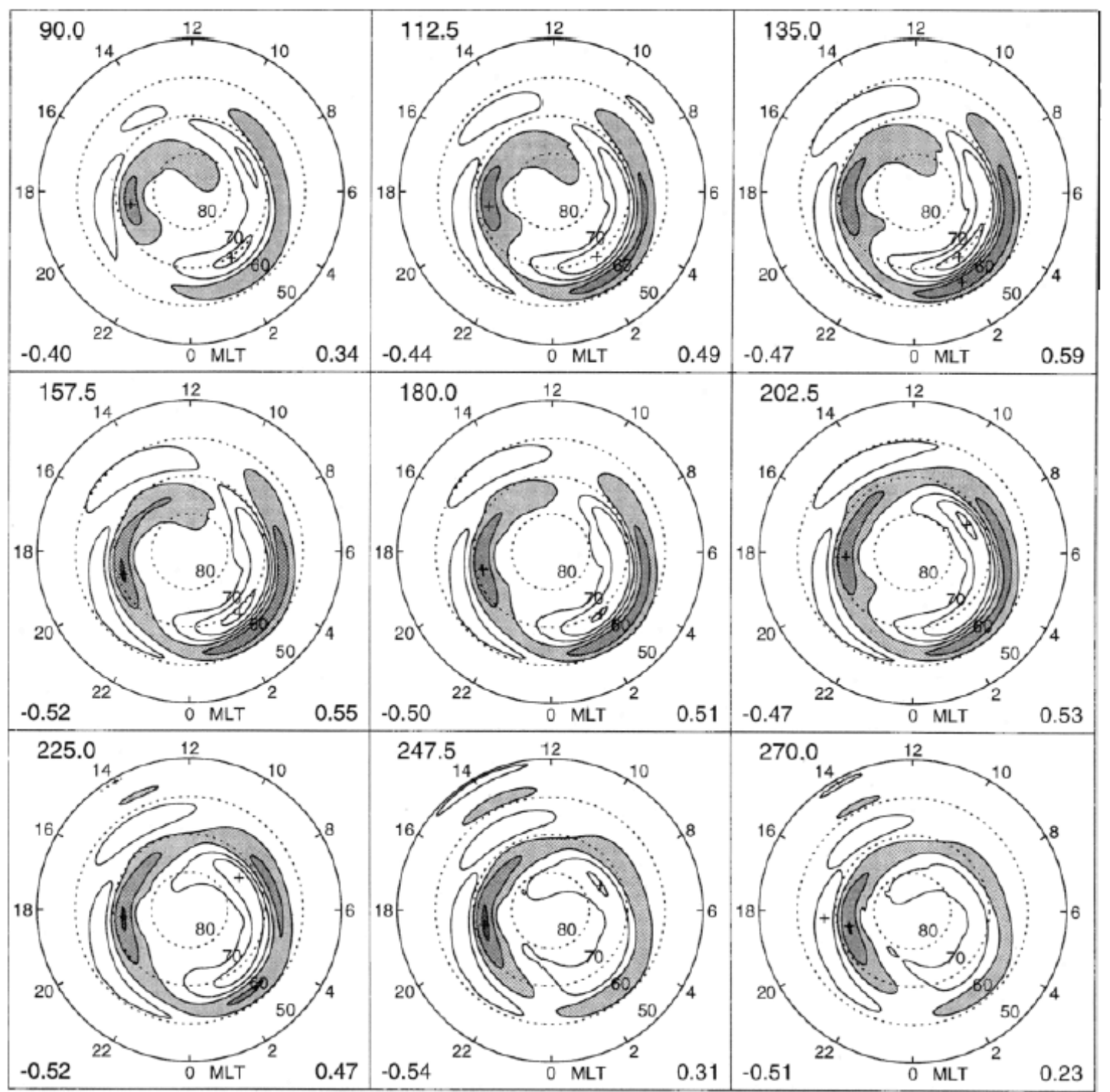
(h)

Ahn et al. [1998] results at top, compared with Hardy et al. [1987] results, bottom.

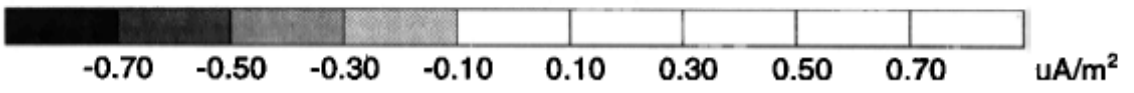
The Hardy et al. [1987] model produces (mostly) reasonable looking current patterns when combined with the W96 electric potential model.



Hardy model with  $K_p=3-$



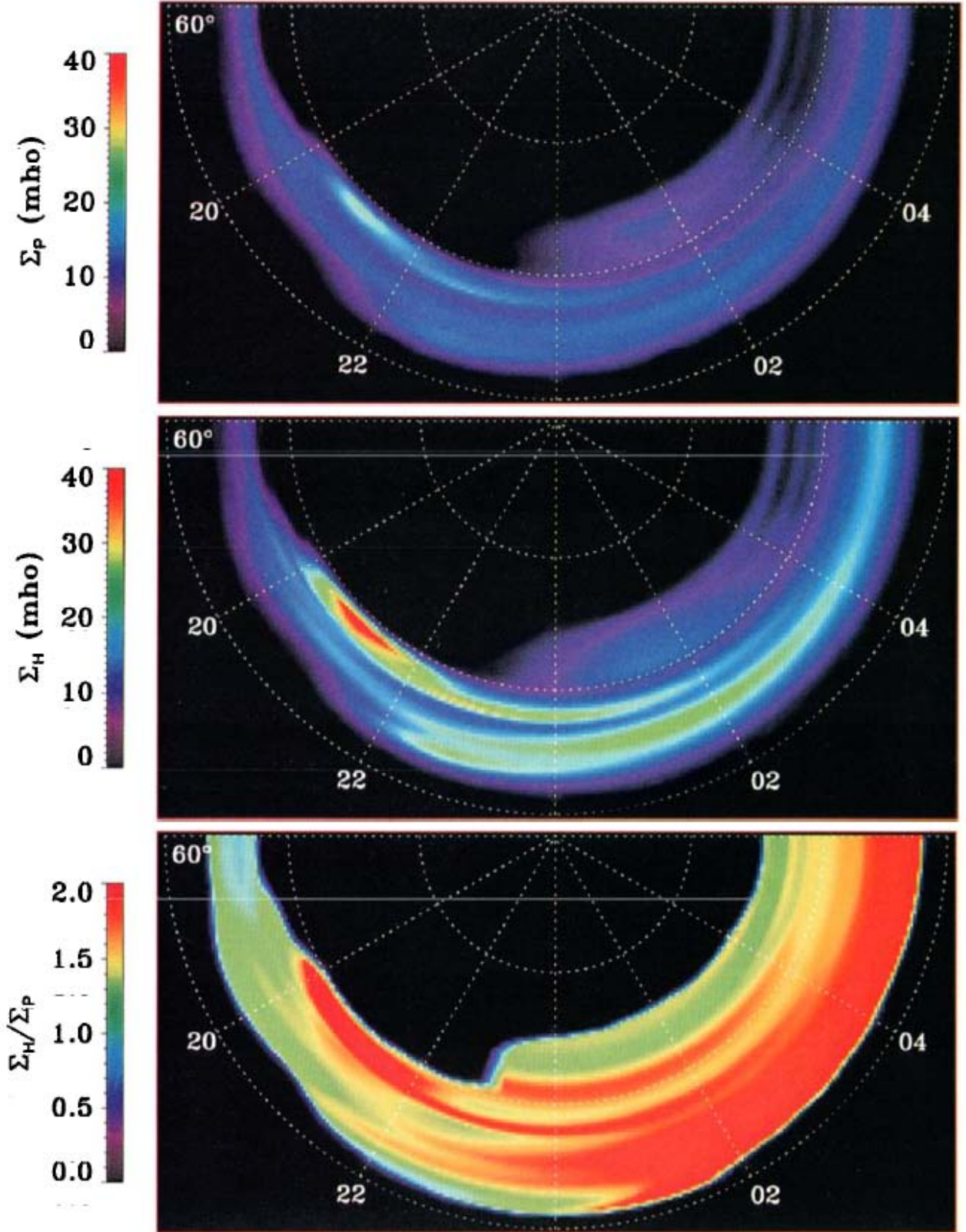
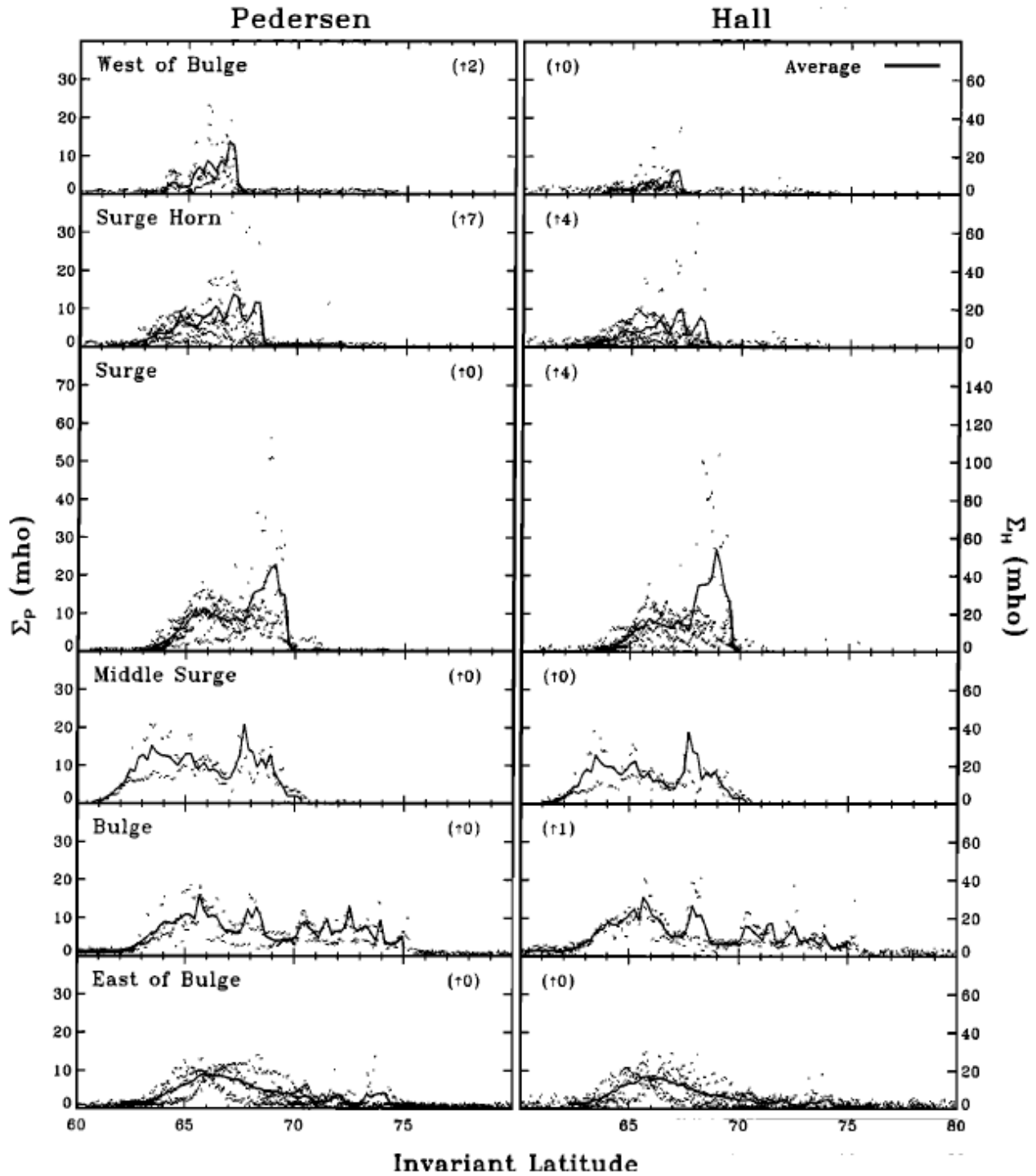
Weimer [1999]



But from personal experience, the combination is known to be terrible for predicting geomagnetic variations at the ground!

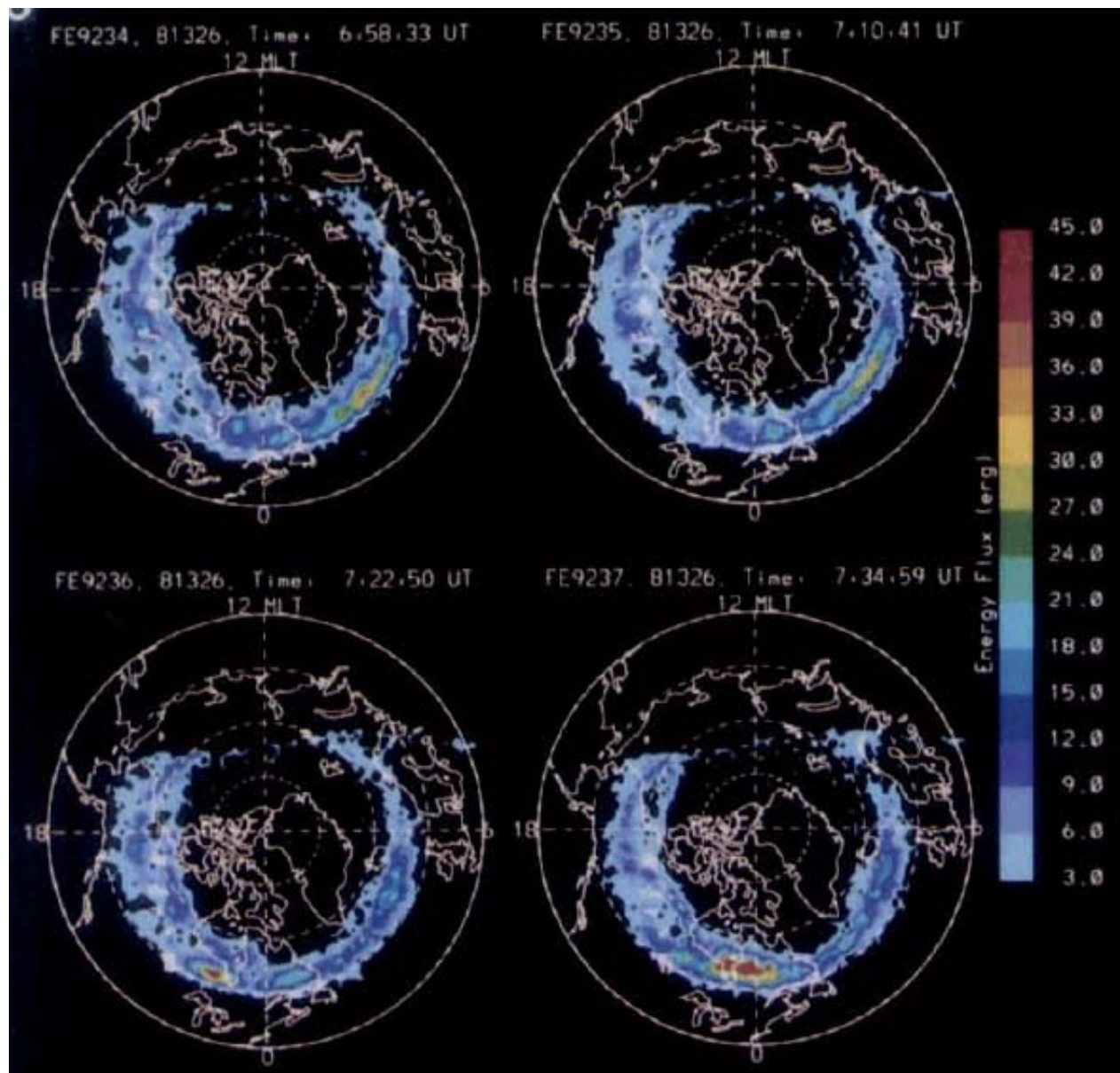
Gjeroloev and Hoffman [2000] looked at conductivity within auroral substorms

DE-2 electron precipitation measurements, sorted by DE-1 imaging, used in a monoenergetic conductance model [Reiff, 1984]

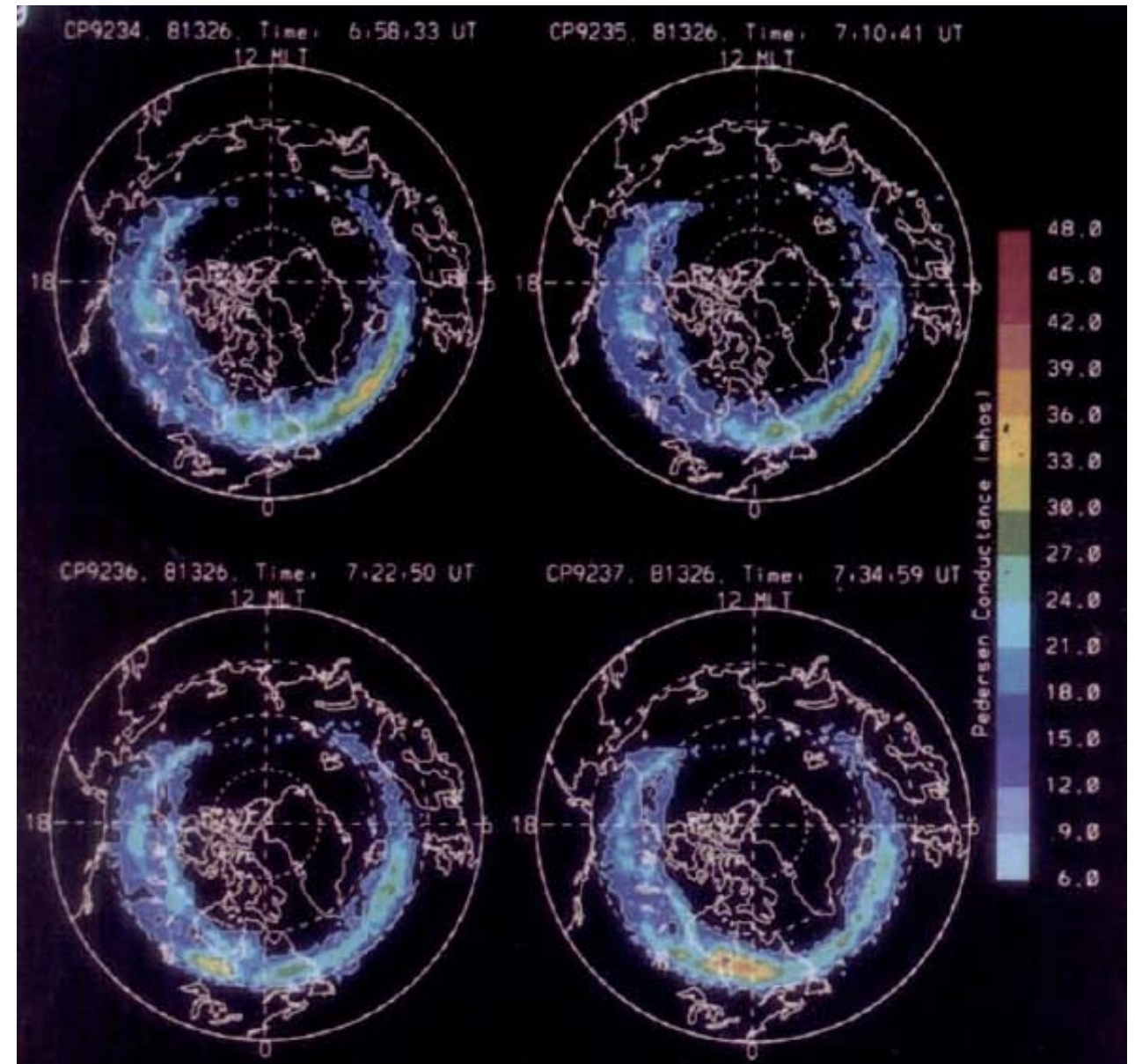


Lummerzheim et al. [1991]: Multispectral auroral images from the Dynamics Explorer satellite used to construct maps of auroral electron energy deposition, mean energy, and ionospheric conductances. An auroral model is used to infer conductances from brightness ratios of different spectral emissions.

## Energy Flux



## Pedersen Conductivity



Green et al. [2007] used data from SuperDARN, DMSP, Iridium, Oersted, and ground magnetometers

$\vec{J}_{df}$  From Ground-Based Magnetometer Data

$\vec{J}_{cf}$  From Iridium, DMSP, and Oersted Data

$\vec{E}_{\perp}$  From Combined SuperDARN and DMSP Data

$$\Sigma_H = \frac{\hat{r} \cdot (\vec{J}_{\perp} \times \vec{E}_{\perp})}{|\vec{E}_{\perp}|^2} \quad \Sigma_P = \frac{\vec{J}_{\perp} \cdot \vec{E}_{\perp}}{|\vec{E}_{\perp}|^2}$$

( Formula from Amm [2001] )

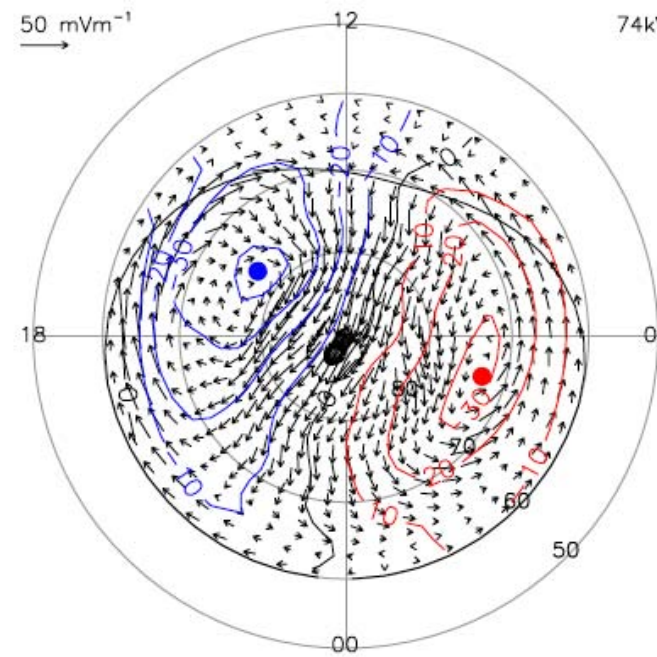


Figure 7. Electric field (rotated by 90° counter clockwise) resulting from the merging of  $\vec{E}_{\perp}$  and  $\vec{E}_{\perp}^{DMSP}$  data in Figure 6.

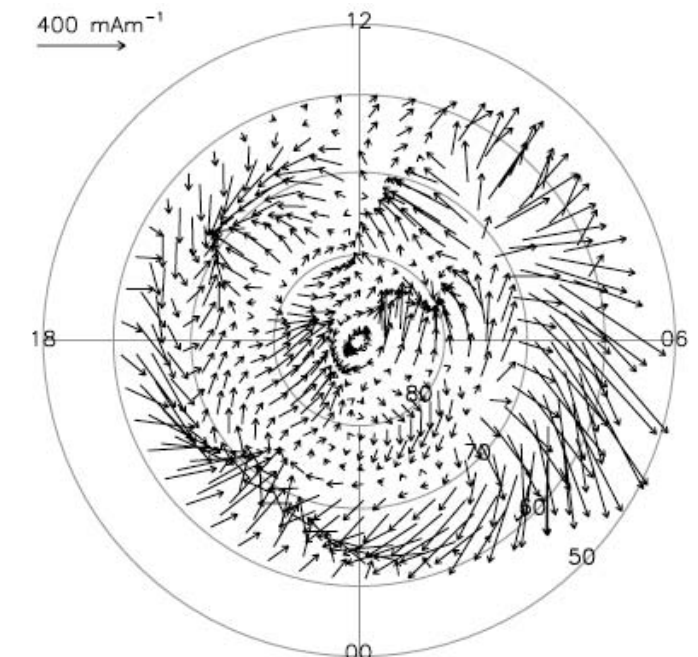


Figure 8.  $\vec{J}_{\perp}$  constructed from the addition of  $\vec{J}_{df}$  (Figure 5) and  $\vec{J}_{cf}$  (Figure 3).

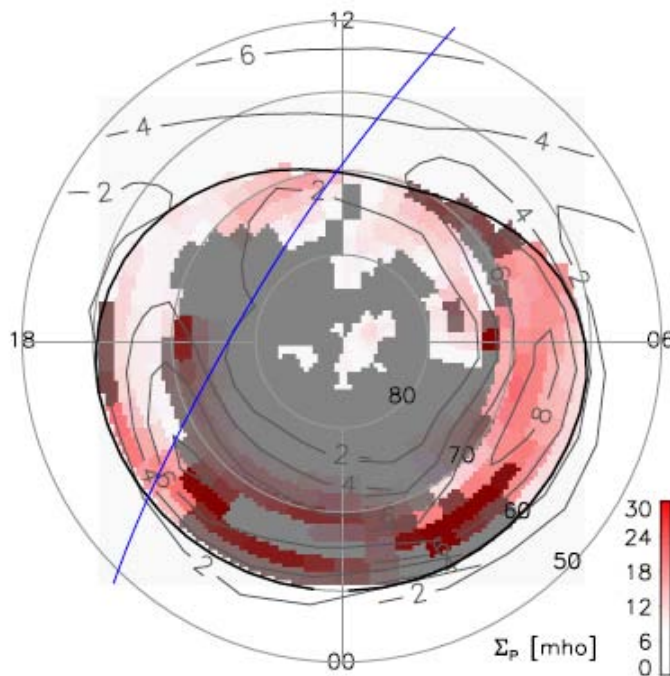


Figure 9. Pedersen conductance calculated from  $\vec{J}_{\perp}$  (Figure 8) and  $\vec{E}_{\perp}$  (Figure 7) for 1 November 2001 0330–0430 UT. Model conductance contours are overlaid. The blue line indicates the path of the F15 DMSP satellite. Grey masking indicates regions of high uncertainty due to variability in the time-averaged electric field.

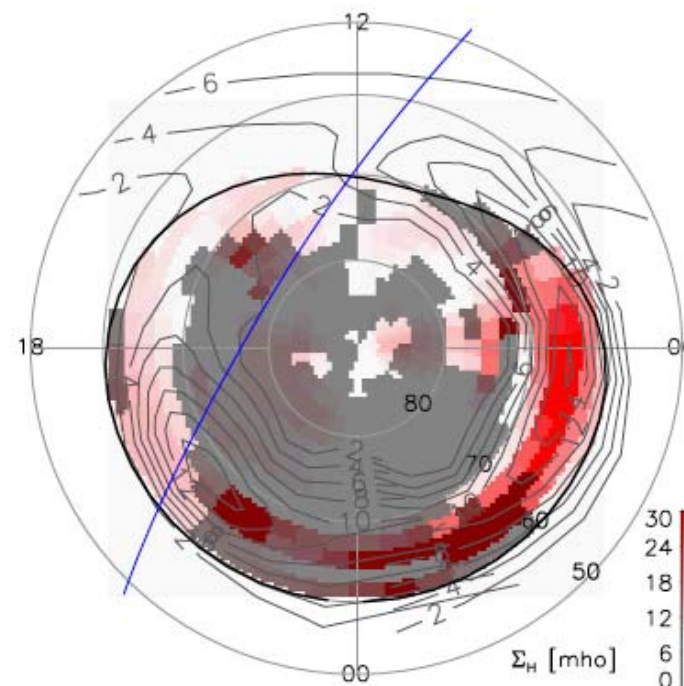
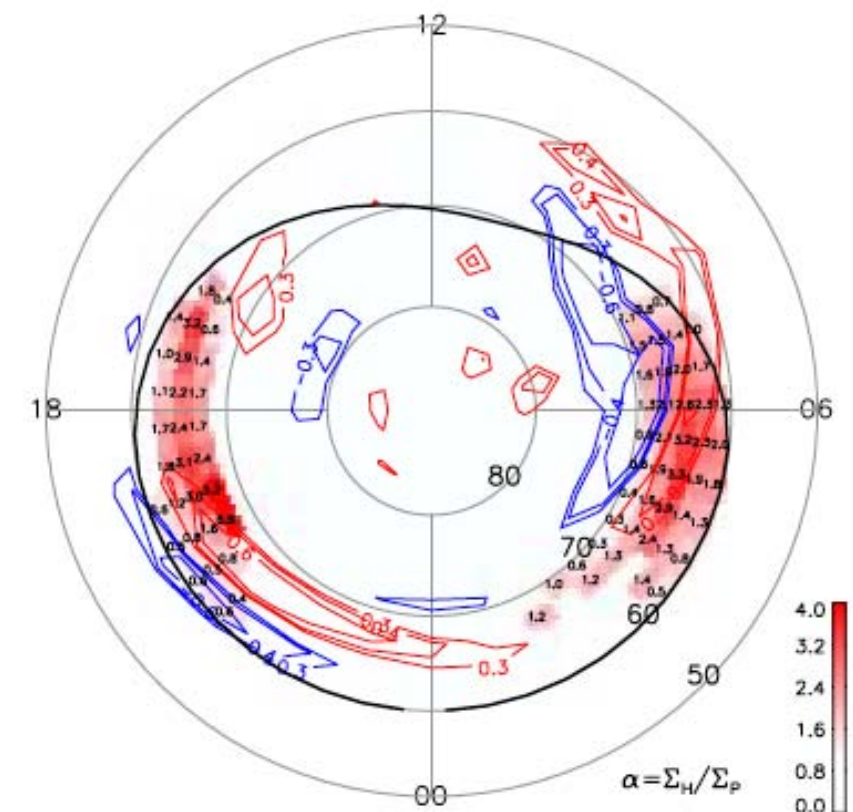
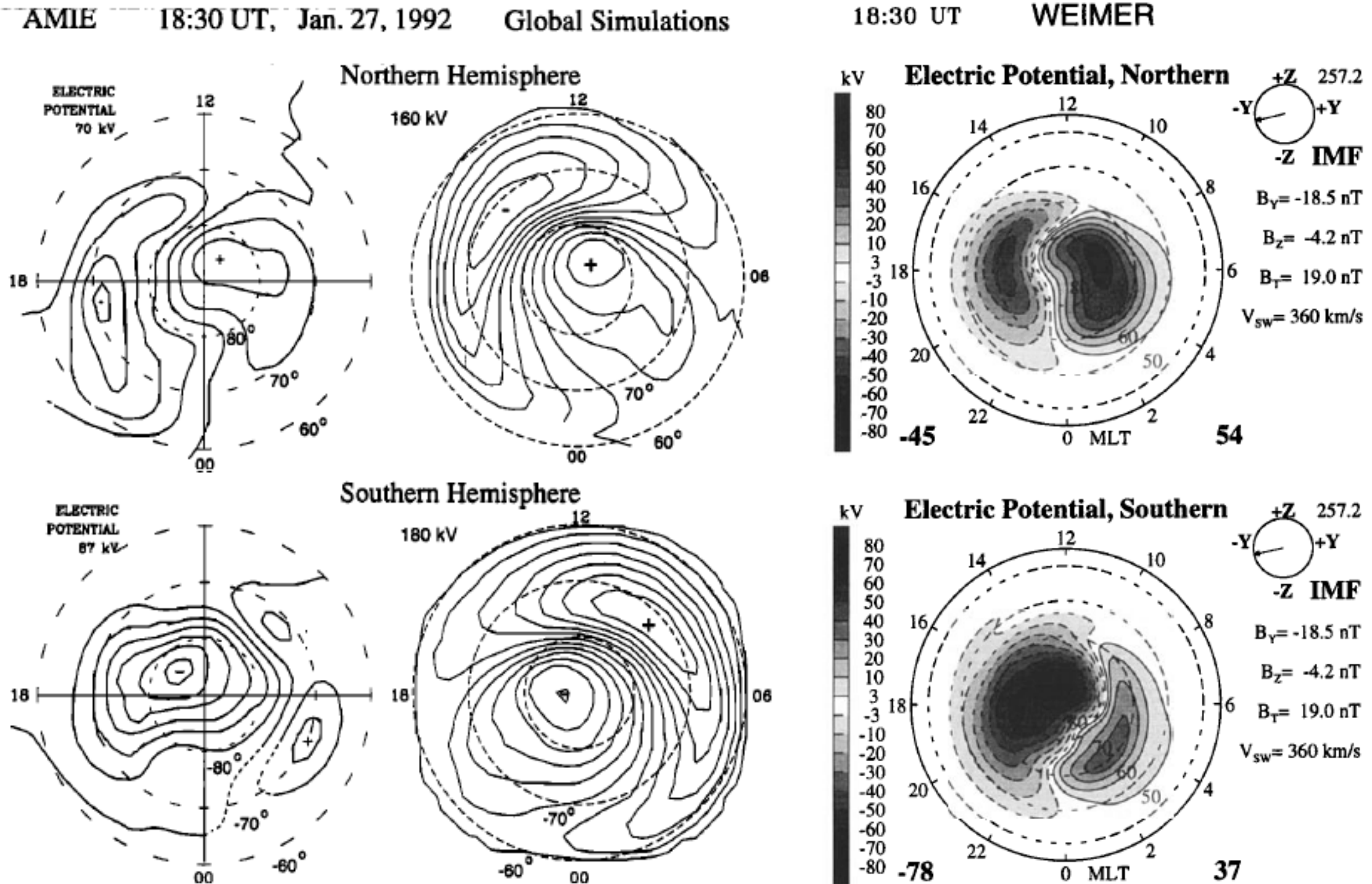


Figure 10. Hall conductance calculated from  $\vec{J}_{\perp}$  (Figure 8) and  $\vec{E}_{\perp}$  (Figure 7) for 1 November 2001 0330–0430 UT.



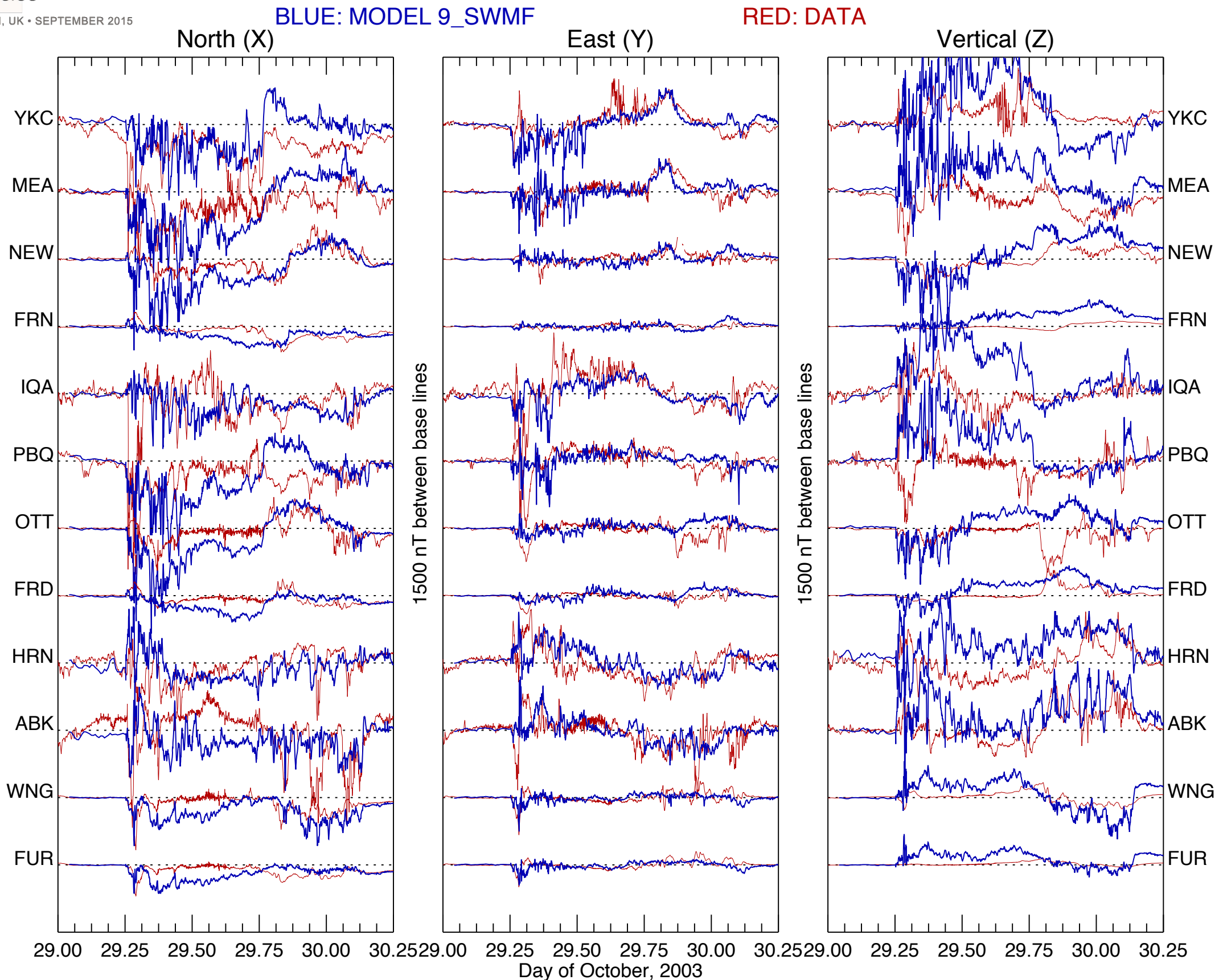
The AMIE technique has often produced electric potentials that are too low, likely due to using conductivity values too high.

MHD models had often produced electric potentials that are too high, (more so in the past), perhaps using conductivity too low.



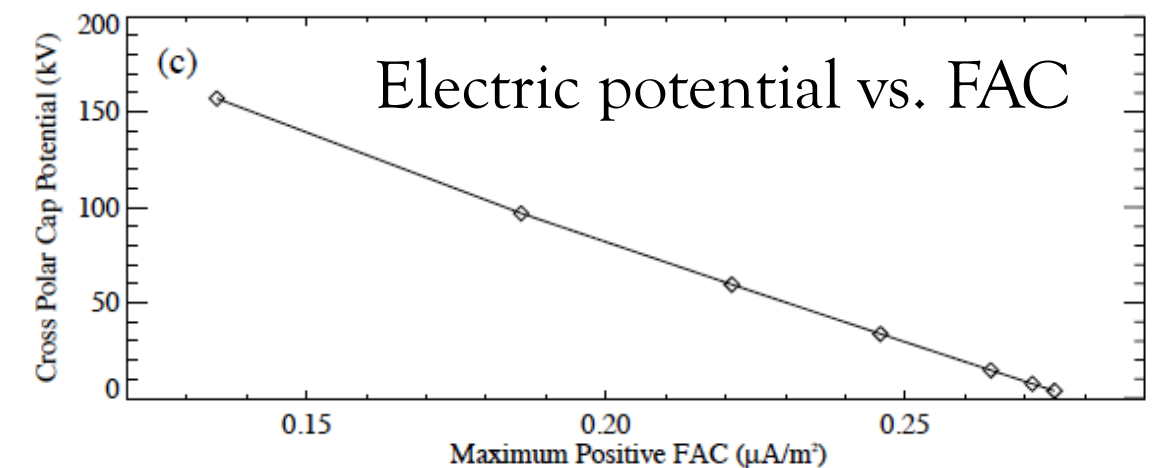
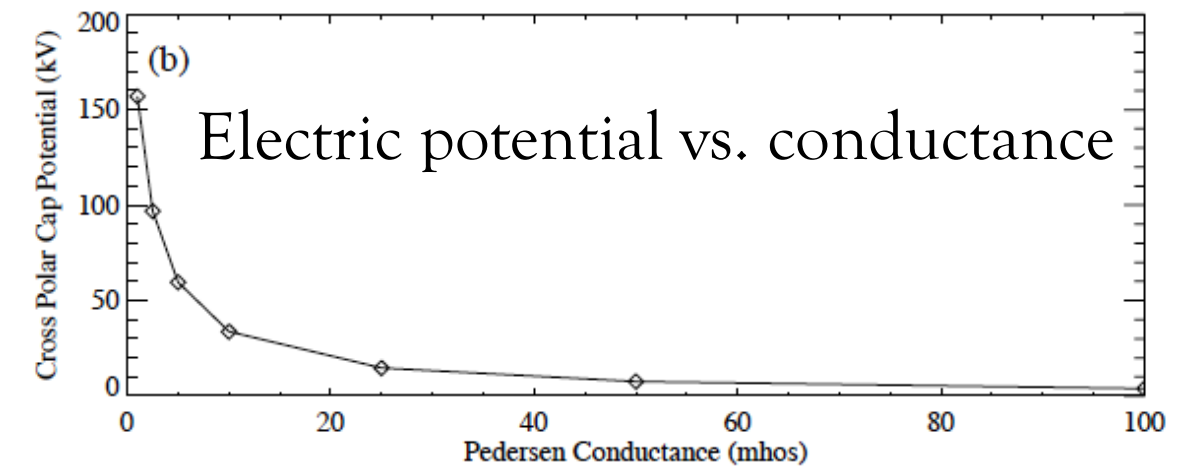
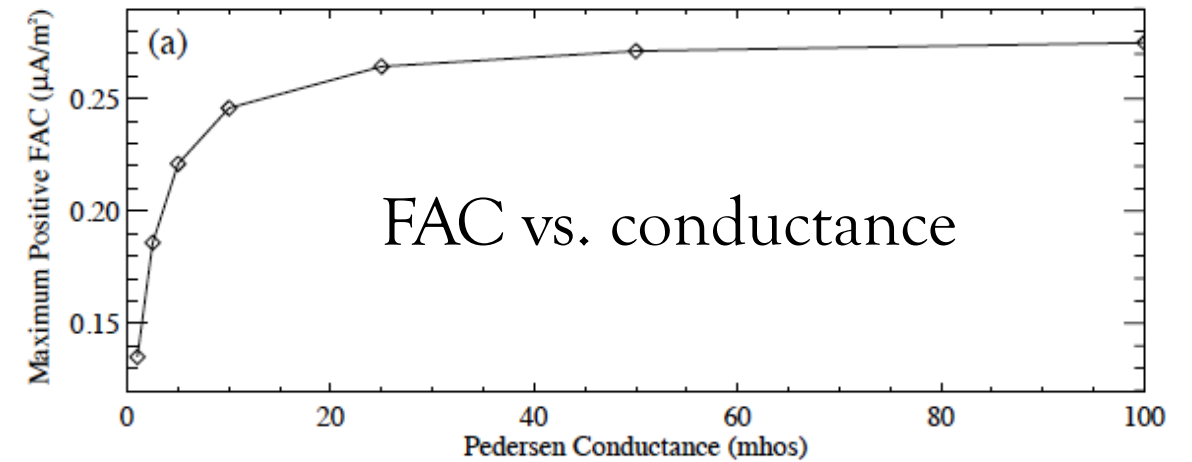
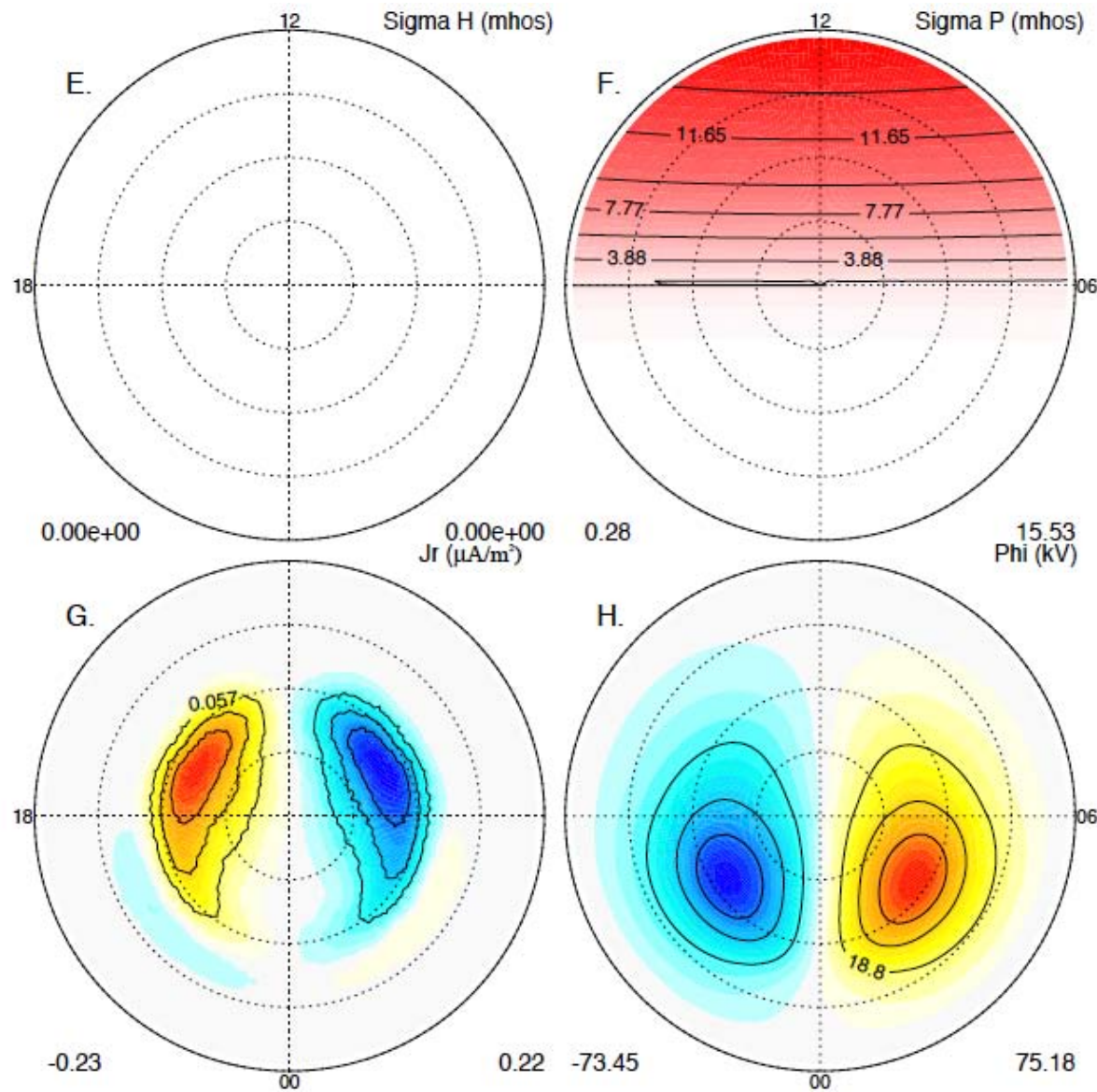
Winglee et al., 1997

Yet, even today the most advanced MHD codes seem to be stymied by difficulties in getting the ionospheric conductivity right.



SWMF computations by CCMC [Pulkkinen et al., 2013], plots by author.

# How does the conductance of the ionosphere control the magnetosphere?



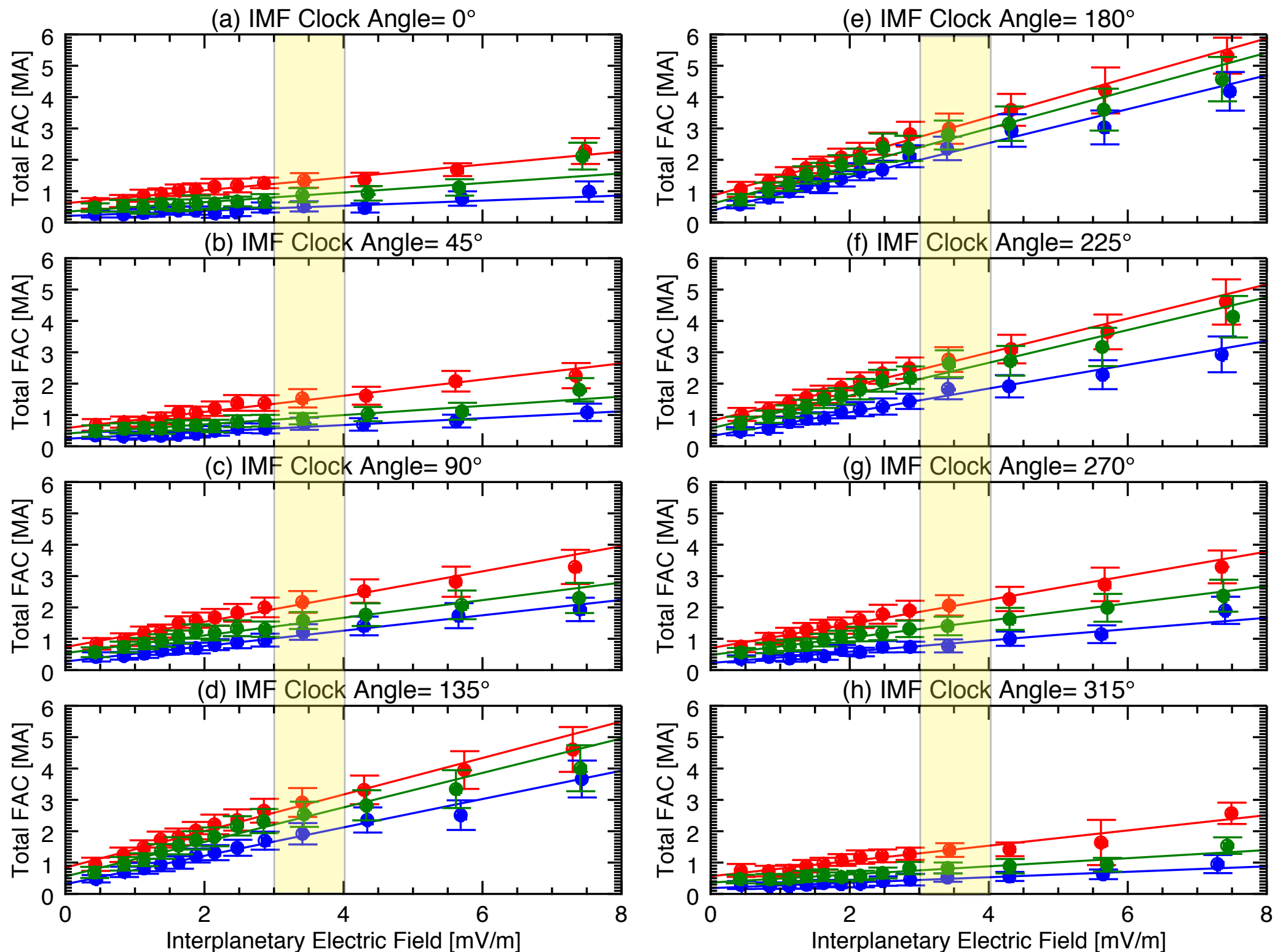
From [Ridley et al. \[2004\]](#), results from MHD model

Total FAC vs. IEF curve is linear far beyond the range where the electric potential saturation effect appears. What is the role of ionospheric conductivity here?

Mean Dawn and Dusk Region 0 and 1 Current vs. IEF

red: summer  
 green: equinox  
 blue: winter

3 to 4 mV/m:  
 range where  
 electric  
 potential  
 saturation  
 begins



# Unsolved Questions (or perhaps never asked)

How do inter-hemispheric differences in ionospheric conductivity affect solar wind coupling to, or within, the magnetosphere and ionosphere?

How does the total conductive "load" of the ionosphere that is presented to the magnetosphere vary with season?

At equinox, with both poles equally illuminated, is the total "parallel" resistance different from solstices, when one pole has a higher conductivity, and the other is lower? Can changes in the total conductance affect some phenomena such as substorm periodicity?

Or does it not matter?

# Summary

We know a lot about the ionosphere's conductance.

A large number of studies done, using different techniques.

Likewise, a large number of different results achieved.

So maybe we don't know so much after all. Conductivity may be the least, well-quantified variable in the system.

What is needed within the community is a comprehensive conductivity model, with software code provided. Needs to use IMF values, not just  $K_p$ . It likely would be better to use EUV indices, rather than  $F_{10.7}$ .

How variability of the ionosphere influences the interaction with the magnetosphere is not well known, and is an unsolved problem.